Iraqi Journal of Science, 2022, Vol. 63, No. 4, pp: 1606-1626
DOI: 10.24996/ijs.2022.63.4.20

ISSN: 0067-2904

Geochemistry of the Middle Eocene Gercus Sandstone, Shaqlawa Area, Northern Iraq: Implications for Provenance, Tectonic Setting and Paleoweathering

Abbas R. Ali[1]*, Omar A. M. Mohammad[2, 3], Mustafa S. Ahmed[2]
[1]*Department of Geography, College of Education for humanities Science, University of Kirkuk, Kirkuk, Iraq*
[2]*Department of Applied Geology, College of Science, University of Kirkuk, Kirkuk, Iraq*
[3]*School of Earth, Atmospheric and Life Sciences, University of Wollongong, Wollongong, Australia*

Received: 2/10/2021 Accepted: 19/12/2021 Published: 30/4/2022

Abstract

The study of the geochemical characterization of sandstone rocks contributes to understand the nature of the source rocks, their tectonic setting and the effects of paleoclimate and paleo-weathering. Accordingly, twenty sandstone samples from the red sandstone units of the Gercus Formation were collected from the northeastern limb of Safin Anticline at Shaqlawa Area – Northern Iraq. The studied sandstone samples show depletion in major, trace elements contents, except for CaO, MgO and Ni, Co and Cr respectively, and general depletion in the rare earth elements (REE) contents. Major element geochemistry indicates that the red bed sandstones of the Gercus Formation are of an oceanic island arc (OIA) tectonic setting. On the other hand, the results revealed that the paleo-weathering of the source area of the Gercus Formation experienced intensive chemical weathering under humid and/or warm climate conditions. The maturity and paleoclimate conclusions of the studied samples suggest a low feldspar content and low values of K_2O / Al_2O_3 ratio, which in turn resulted from the dominance of low grade metamorphic and sedimentary rock types in the source area.

Keywords: Geochemistry; Sedimentary provenance; Oceanic Island Arc (OIA); Siliciclastic; Middle Eocene.

جيوكيميائية الحجر الرملي لتكوين جركس (الايوسين الاوسط), منطقة شقلاوة, شمالي شرقي العراق: تطبيقات في المصدرية، الموقع التكتوني والتجوية القديمة

عباس رشيد علي[1]*, عمر عادل محمد[2, 3], مصطفى شهاب احمد[2]

[1]قسم الجغرافية, كلية التربية للعلوم الانسانية, جامعة كركوك, كركوك, العراق

[2]قسم الجيولوجيا التطبيقية, كلية العلوم, جامعة كركوك, كركوك العراق

[3]قسم علوم الارض, الجو والحياة, جامعة وولنغونغ, وولنغونغ, استراليا

---

* Email: abbaskervanci@uokirkuk.edu.iq

الخلاصة

تساهم دراسة التوصيف الجيوكيميائي لصخور الحجر الرملي في فهم طبيعة صخور المصدر, وضعها التكتوني وتاثيرات المناخ القديم والتجوية عليها. وفقا لهذا, تم جمع عشرين عينة من وحدات الحجر الرملي الحمراء لتكوين جركس من الجناح الشمالي الشرقي لطية سفين ضمن منطقة شقلاوة – شمالي العراق. اظهرت عينات الحجر الرملي نضوبًا في محتواها من العناصر الرئيسة والاثرية باستثناء CaO، MgO و Ni، Co، Cr على التوالي و نضوبا عاما في محتوى العناصر الأرضية النادرة (REE). تشير جيوكيميائية العناصر الرئيسة أن طبقات الحجر الرملي الحمراء لتكوين جركس ناجمة عن الوضع التكتوني لاقواس الجزر المحيطية (OIA). وان التجوية القديمة في منطقة المصدر لتكوين جركس عانت من التجوية الكيميائية المكثفة تحت ظروف مناخية رطبة و/أو دافئة. كما تشير نتائج النضوجية والمناخ القديم للعينات المدروسة إلى انخفاض محتوى الفلدسبار و نسبة K_2O/Al_2O_3 المنخفضة والتي نتجت بدورها عن طبيعة صخور المصدر والتي تشتمل على الصخور المتحولة واطئة التحول والصخور الرسوبية.

1. Introduction

Several geologic branches utilize provenance analysis in their study to correlate and evaluate rock units for energy resources. Petrographic studies of siliciclastic rocks were implemented in the provenance studies by many authors to understand source rock type, tectonic setting, paleo-weathering, paleoclimate and paleogeographic. Further, sandstone geochemistry was implemented in many studies worldwide to delineate the sedimentological history of the sediments cycling and maturation through geologic time. The geochemistry of sedimentary rocks is genetically linked to the mineralogical assemblages of the rocks and, therefore, have been used to understand weathering, diagenesis and, of course provenance [1]. On the other hand, rare earth geochemistry is used to understand the sediment recycling and maturation because it provides a unique tool to explore the ancient history of the sediments. Trace and rare earth elements (REE) are relatively reliable more than significant in understanding the provenance and the tectonic setting and identifying the felsic or mafic contribution in the source area [2, 3, 4, 5, 6, 7].

Insight from geochemistry can better understand the different factors that control sediment differentiation and maturation and thus changes in the whole rock geochemistry. This paper aims to utilize sandstone geochemistry to understand the source area characteristics and framework of the tectonic setting, provenance, and paleo-weathering of sandstone of the Gercus Formation in northeastern Iraq.

2. Geological Setting

Shaqlawa city is located in northeastern Erbil Governorate (Figure 1) and represent an accessible area to carry out the study. The studied section is located in the northeast limb of Safin Anticline, representing northwestern- southeastern trend double plunging asymmetrical anticline fold. Safin anticline is situated in the High Folded Zone in the Unstable Shelf of The Arabian Plate [8, 9].

Red sandstone of the Gercus Formation is targeted in previous works to clarify the geochemical analysis's role and study major trace and rare earth elements in understanding provenance and its implication [10- 21].

Middle Eocene, the Gercus Formation, first described by Maxson (1936) SE Turkey while a supplementary type section was chosen in Iraq in Dohuk [21]. The Middle Eocene age is assigned to the formation because of the stratigraphic position and some scarce palynomorphs data [22]. The stratigraphic position of the formation is well known to be placed between the Pila Spi and Kolosh formations.

The stratigraphic formation relationships are deferential locally from comfortable to uncomfortable, especially in northeastern Iraq where conglomerate beds are observable [15, 21, 23, 24]. The lower boundary with Kolosh Formation is generally gradational [8, 25] and locally unconformable [23, 16, 21]. At the same time, it is gradational with the Khurmala

Formation [15, 24, 25] and Sinjar Formation [26] with local scale unconformity [27]. The upper contact surface between Gercus and Pila Spi Formations is gradational [8], while other authors reported conformable and unconformable relationships [16, 23, 24].

The formation's lithology is composed mainly ofof siliciclastic rocks with some limestone, dolomitic limestone, gypsum [17] and black shale with a rarely described igneous intrusion [20]. Conglomerate beds occurrence refers to local unconformity stratigraphic relationships of the formation. It could reach 20 m near Dohuk Area and 6 m in the upper part of the Gercus Formation near Shaqlawa City [7]. Argillaceous shale is reported from locations, especially in Koisanjak city northeastern Iraq [10]. The red pigment is a unique and common feature in the Gercus Formation throughout the outcropped formation area in the north- northeastern Iraq area. Several studies studied the geochemistry and mineralogy (please refer to [7] and references within) of the Gercus Formation, including the red pigments [14, 28, 29]. Further, the formation thickness is ranged from less than 100 m in the northeast to several hundred meters in northern Iraq (i.e. 800 m in Dohuk Area) [19].

The siliciclastic rocks of the Gercus Formation show a variety of sedimentary environments from aeolian, fluvial, lacustrine [18] and marine sedimentary environments [11]. This is evident from the fluviatile with arid to semi-arid climate [14], clastic dominated tidal flat [12] and gravity flow regime in the marine environment [11]. On the other hand, delta and delta front depositional environment with some sedimentary structures refer to braided delta, with minor intertidal and supratidal environments intercalation [16].

3. Stratigraphic description

The studied section is approximately 28 m, representing the outcropped part of the formation in the studded area. The section alternates between sandstone and claystone, with two thick beds of silty claystone and 1.5 m of dolomitic limestone at the top of the section (Figure1).

The section is outcropped with first relatively thick sandstones layers, which reach more than 1m. The contact surfaces between the sandstone layers are fairly obvious. A thin mudstone (claystone) layer alternates the thick sandstone layer. This continued until the first thick silty claystone layer appeared near the mid of the section (Figure1). The thick silty claystone seems to reflect the gradual fining upward sequence as a 5.5-m-thick mudstone bed appears at the top of the thick silty claystone bed with a nearly recognized contact surface.

This pattern continues following the thick mudstone bed, with the reappearance of the silty claystone layer that reaches 2 m. After this point, 4 m thick mudstone beds outcrop with obvious contact surface with the alternate sandstone layer. A mudstone bed with a 1-m thickness succeeds the last sandstones layer in the section. It is ending up with a very interesting 1-m-thick dolomitic limestone at the top of the examined section.

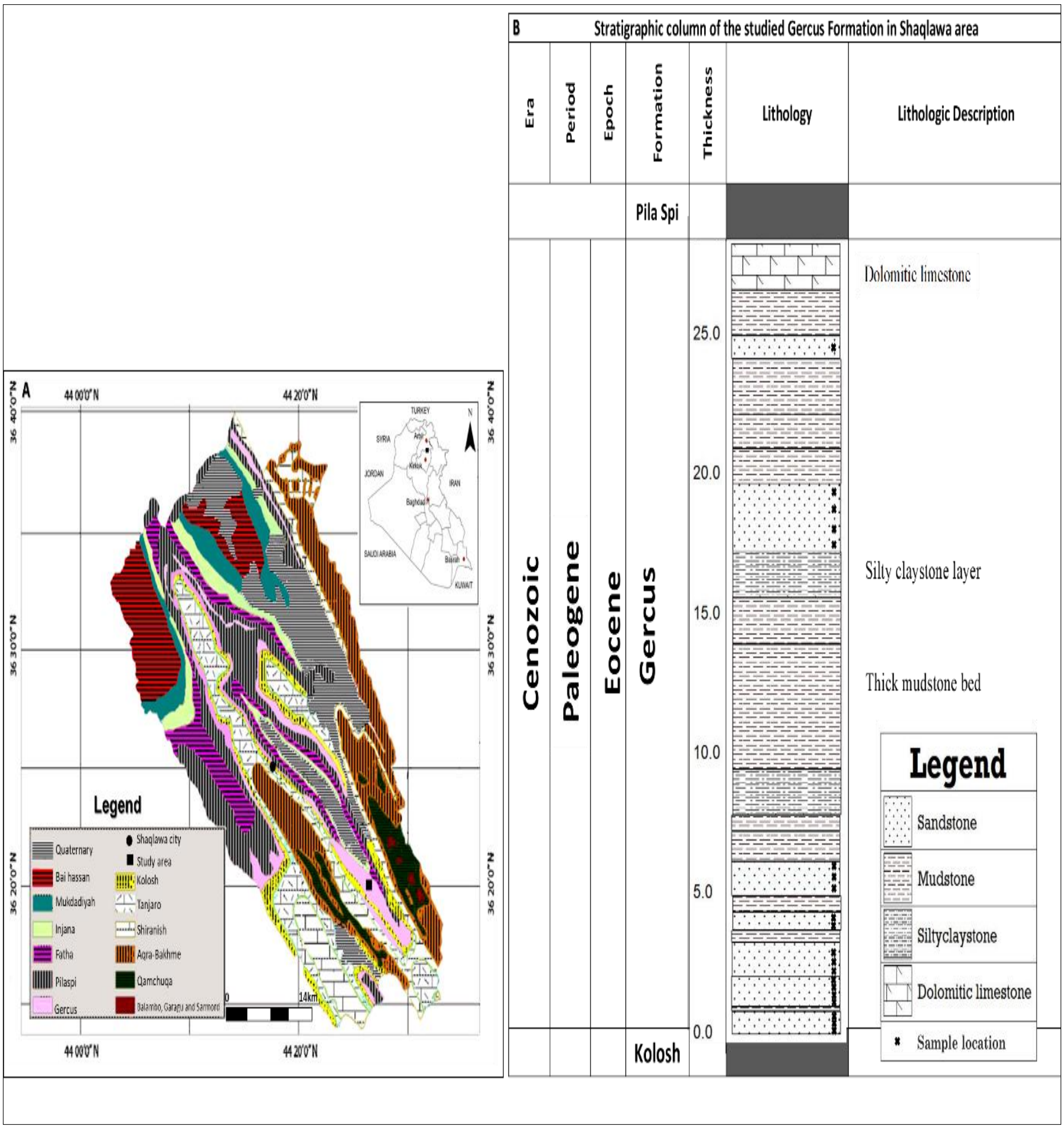

Figure 1-(A): Geological map of the study area after [9], [30]. (B): Representative lithologic section of the studied the Gercus Formation.

4. Materials and Methods

A total of twenty sandstone samples were collected from the studied section of the Gercus Formation at Shaqlawa area – Northern Iraq. The studied samples represent the red sandstones layers systematically within each sedimentary cycle (Figure 1). All samples were subsequently air-dried and prepared for whole-rock geochemistry analysis. Major, trace and the rare earth elements contents were measured using inductively coupled plasma mass spectrometry (ICP-MS) at Bureau Veritas Commodities Canada Ltd. The results and detection limit for each element are given in Table1.

Table 1 Whole-rock geochemistry of the siliciclastic rock samples of the Gercus Formation.

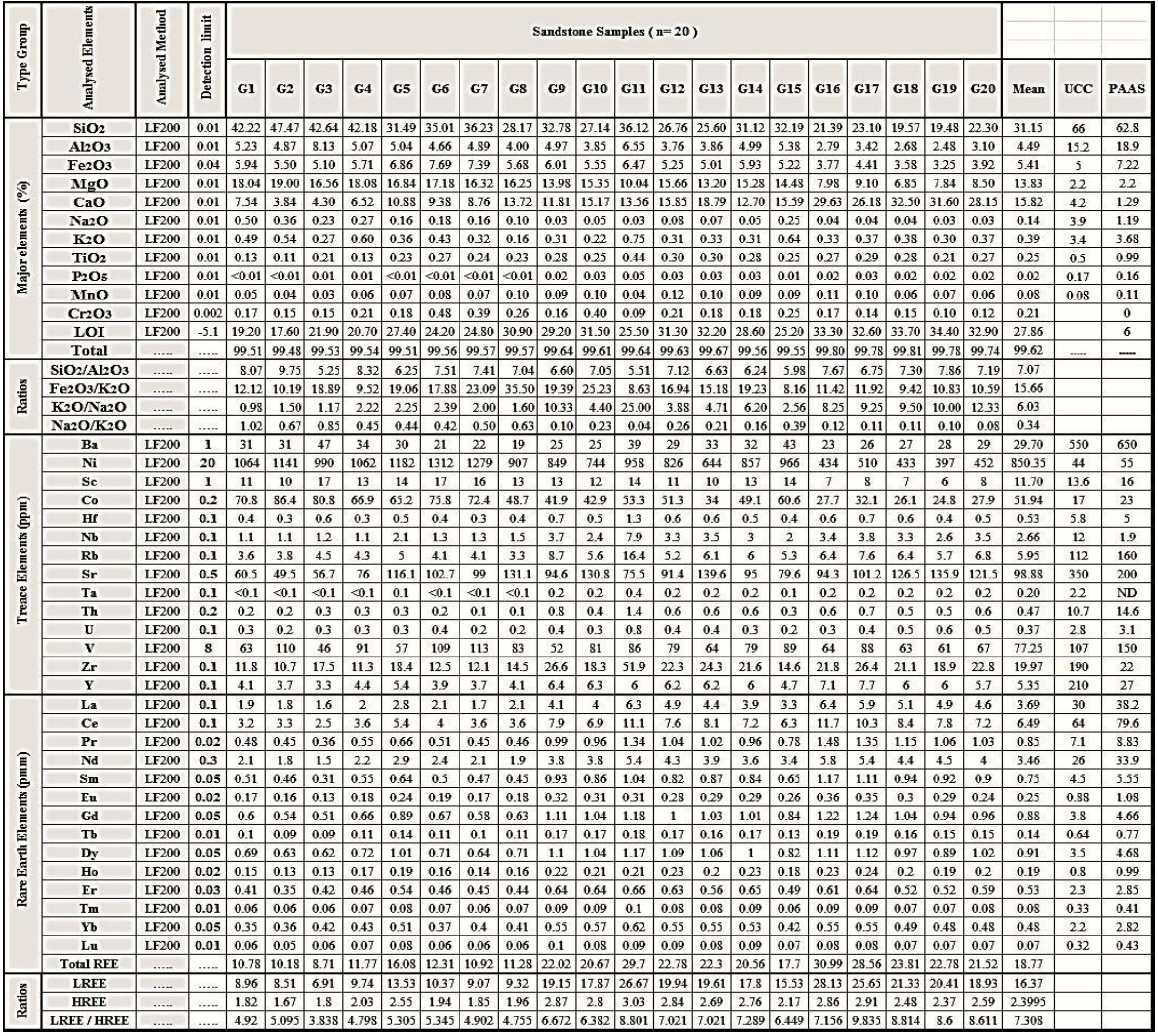

Type Group	Analysed Elements	Analysed Method	Detection limit	Sandstone Samples (n= 20)																						
				G1	G2	G3	G4	G5	G6	G7	G8	G9	G10	G11	G12	G13	G14	G15	G16	G17	G18	G19	G20	Mean	UCC	PAAS
Major elements (%)	SiO_2	LF200	0.01	42.22	47.47	42.64	42.18	31.49	35.01	36.23	28.17	32.78	27.14	36.12	26.76	25.60	31.12	32.19	21.39	23.10	19.57	19.48	22.30	31.15	66	62.8
	Al_2O_3	LF200	0.01	5.23	4.87	8.13	5.07	5.04	4.66	4.89	4.00	4.97	3.85	6.55	3.76	3.86	4.99	5.38	2.79	3.42	2.68	2.48	3.10	4.49	15.2	18.9
	Fe_2O_3	LF200	0.04	5.94	5.50	5.10	5.71	6.86	7.69	7.39	5.68	6.01	5.55	6.47	5.25	5.01	5.93	5.22	3.77	4.41	3.58	3.25	3.92	5.41	5	7.22
	MgO	LF200	0.01	18.04	19.00	16.56	18.08	16.84	17.18	16.32	16.25	13.98	15.35	10.04	15.66	13.20	15.28	14.48	7.98	9.10	6.85	7.84	8.50	13.83	2.2	2.2
	CaO	LF200	0.01	7.54	3.84	4.30	6.52	10.88	9.38	8.76	13.72	11.81	15.17	13.56	15.85	18.79	12.70	15.59	29.63	26.18	32.50	31.60	28.15	15.82	4.2	1.29
	Na_2O	LF200	0.01	0.50	0.36	0.23	0.27	0.16	0.18	0.16	0.10	0.03	0.05	0.03	0.08	0.07	0.05	0.25	0.04	0.04	0.04	0.03	0.03	0.14	3.9	1.19
	K_2O	LF200	0.01	0.49	0.54	0.27	0.60	0.36	0.43	0.32	0.16	0.31	0.22	0.75	0.31	0.33	0.31	0.64	0.33	0.37	0.38	0.30	0.37	0.39	3.4	3.68
	TiO_2	LF200	0.01	0.13	0.11	0.21	0.13	0.23	0.27	0.24	0.23	0.28	0.25	0.44	0.30	0.30	0.28	0.25	0.27	0.29	0.28	0.21	0.27	0.25	0.5	0.99
	P_2O_5	LF200	0.01	<0.01	<0.01	0.01	0.01	<0.01	<0.01	<0.01	<0.01	0.02	0.03	0.05	0.03	0.03	0.03	0.01	0.02	0.03	0.02	0.02	0.02	0.02	0.17	0.16
	MnO	LF200	0.01	0.05	0.04	0.03	0.06	0.07	0.08	0.07	0.10	0.09	0.10	0.04	0.12	0.10	0.09	0.09	0.11	0.10	0.06	0.07	0.06	0.08	0.08	0.11
	Cr_2O_3	LF200	0.002	0.17	0.15	0.15	0.21	0.18	0.48	0.39	0.26	0.16	0.40	0.09	0.21	0.18	0.18	0.25	0.17	0.14	0.15	0.10	0.12	0.21		0
	LOI	LF200	-5.1	19.20	17.60	21.90	20.70	27.40	24.20	24.80	30.90	29.20	31.50	25.50	31.30	32.20	28.60	25.20	33.30	32.60	33.70	34.40	32.90	27.86		6
	Total	…..	…..	99.51	99.48	99.53	99.54	99.51	99.56	99.57	99.57	99.64	99.61	99.64	99.63	99.67	99.56	99.55	99.80	99.78	99.81	99.78	99.74	99.62	…..	----
Ratios	SiO_2/Al_2O_3	…..	…..	8.07	9.75	5.25	8.32	6.25	7.51	7.41	7.04	6.60	7.05	5.51	7.12	6.63	6.24	5.98	7.67	6.75	7.30	7.86	7.19	7.07		
	Fe_2O_3/K_2O	…..	…..	12.12	10.19	18.89	9.52	19.06	17.88	23.09	35.50	19.39	25.23	8.63	16.94	15.18	19.23	8.16	11.42	11.92	9.42	10.83	10.59	15.66		
	K_2O/Na_2O	…..	…..	0.98	1.50	1.17	2.22	2.25	2.39	2.00	1.60	10.33	4.40	25.00	3.88	4.71	6.20	2.56	8.25	9.25	9.50	10.00	12.33	6.03		
	Na_2O/K_2O	…..	…..	1.02	0.67	0.85	0.45	0.44	0.42	0.50	0.63	0.10	0.23	0.04	0.26	0.21	0.16	0.39	0.12	0.11	0.11	0.10	0.08	0.34		
Treace Elements (ppm)	Ba	LF200	1	31	31	47	34	30	21	22	19	25	25	39	29	33	32	43	23	26	27	28	29	29.70	550	650
	Ni	LF200	20	1064	1141	990	1062	1182	1312	1279	907	849	744	958	826	644	857	966	434	510	433	397	452	850.35	44	55
	Sc	LF200	1	11	10	17	13	14	17	16	13	13	12	14	11	10	13	14	7	8	7	6	8	11.70	13.6	16
	Co	LF200	0.2	70.8	86.4	80.8	66.9	65.2	75.8	72.4	48.7	41.9	42.9	53.3	51.3	34	49.1	60.6	27.7	32.1	26.1	24.8	27.9	51.94	17	23
	Hf	LF200	0.1	0.4	0.3	0.6	0.3	0.5	0.4	0.3	0.4	0.7	0.5	1.3	0.6	0.6	0.5	0.4	0.6	0.7	0.6	0.4	0.5	0.53	5.8	5
	Nb	LF200	0.1	1.1	1.1	1.2	1.1	2.1	1.3	1.3	1.5	3.7	2.4	7.9	3.3	3.5	3	2	3.4	3.8	3.3	2.6	3.5	2.66	12	1.9
	Rb	LF200	0.1	3.6	3.8	4.5	4.3	5	4.1	4.1	3.3	8.7	5.6	16.4	5.2	6.1	6	5.3	6.4	7.6	6.4	5.7	6.8	5.95	112	160
	Sr	LF200	0.5	60.5	49.5	56.7	76	116.1	102.7	99	131.1	94.6	130.8	75.5	91.4	139.6	95	79.6	94.3	101.2	126.5	135.9	121.5	98.88	350	200
	Ta	LF200	0.1	<0.1	<0.1	<0.1	<0.1	0.1	<0.1	<0.1	<0.1	0.2	0.2	0.4	0.2	0.2	0.2	0.1	0.2	0.2	0.2	0.2	0.2	0.20	2.2	ND
	Th	LF200	0.2	0.2	0.2	0.3	0.3	0.3	0.2	0.1	0.1	0.8	0.4	1.4	0.6	0.6	0.6	0.3	0.6	0.7	0.5	0.5	0.6	0.47	10.7	14.6
	U	LF200	0.1	0.3	0.2	0.3	0.3	0.3	0.4	0.2	0.2	0.4	0.3	0.8	0.4	0.4	0.3	0.2	0.3	0.4	0.5	0.6	0.5	0.37	2.8	3.1
	V	LF200	8	63	110	46	91	57	109	113	83	52	81	86	79	64	79	89	64	88	63	61	67	77.25	107	150
	Zr	LF200	0.1	11.8	10.7	17.5	11.3	18.4	12.5	12.1	14.5	26.6	18.3	51.9	22.3	24.3	21.6	14.6	21.8	26.4	21.1	18.9	22.8	19.97	190	22
	Y	LF200	0.1	4.1	3.7	3.3	4.4	5.4	3.9	3.7	4.1	6.4	6.3	6	6.2	6.2	6	4.7	7.1	7.7	6	6	5.7	5.35	210	27
Rare Earth Elements (pmm)	La	LF200	0.1	1.9	1.8	1.6	2	2.8	2.1	1.7	2.1	4.1	4	6.3	4.9	4.4	3.9	3.3	6.4	5.9	5.1	4.9	4.6	3.69	30	38.2
	Ce	LF200	0.1	3.2	3.3	2.5	3.6	5.4	4	3.6	3.6	7.9	6.9	11.1	7.6	8.1	7.2	6.3	11.7	10.3	8.4	7.8	7.2	6.49	64	79.6
	Pr	LF200	0.02	0.48	0.45	0.36	0.55	0.66	0.51	0.45	0.46	0.99	0.96	1.34	1.04	1.02	0.96	0.78	1.48	1.35	1.15	1.06	1.03	0.85	7.1	8.83
	Nd	LF200	0.3	2.1	1.8	1.5	2.2	2.9	2.4	2.1	1.9	3.8	3.8	5.4	4.3	3.9	3.6	3.4	5.8	5.4	4.4	4.5	4	3.46	26	33.9
	Sm	LF200	0.05	0.51	0.46	0.31	0.55	0.64	0.5	0.47	0.45	0.93	0.86	1.04	0.82	0.87	0.84	0.65	1.17	1.11	0.94	0.92	0.9	0.75	4.5	5.55
	Eu	LF200	0.02	0.17	0.16	0.13	0.18	0.24	0.19	0.17	0.18	0.32	0.31	0.31	0.28	0.29	0.29	0.26	0.36	0.35	0.3	0.29	0.24	0.25	0.88	1.08
	Gd	LF200	0.05	0.6	0.54	0.51	0.66	0.89	0.67	0.58	0.63	1.11	1.04	1.18	1	1.03	1.01	0.84	1.22	1.24	1.04	0.94	0.96	0.88	3.8	4.66
	Tb	LF200	0.01	0.1	0.09	0.09	0.11	0.14	0.11	0.1	0.11	0.17	0.17	0.18	0.17	0.16	0.17	0.13	0.19	0.19	0.16	0.15	0.15	0.14	0.64	0.77
	Dy	LF200	0.05	0.69	0.63	0.62	0.72	1.01	0.71	0.64	0.71	1.1	1.04	1.17	1.09	1.06	1	0.82	1.11	1.12	0.97	0.89	1.02	0.91	3.5	4.68
	Ho	LF200	0.02	0.15	0.13	0.13	0.17	0.19	0.16	0.14	0.16	0.22	0.21	0.21	0.23	0.2	0.23	0.18	0.23	0.24	0.2	0.19	0.2	0.19	0.8	0.99
	Er	LF200	0.03	0.41	0.35	0.42	0.46	0.54	0.46	0.45	0.44	0.64	0.64	0.66	0.63	0.56	0.65	0.49	0.61	0.64	0.52	0.52	0.59	0.53	2.3	2.85
	Tm	LF200	0.01	0.06	0.06	0.06	0.07	0.08	0.07	0.06	0.07	0.09	0.09	0.1	0.08	0.08	0.09	0.06	0.09	0.09	0.07	0.07	0.08	0.08	0.33	0.41
	Yb	LF200	0.05	0.35	0.36	0.42	0.43	0.51	0.37	0.4	0.41	0.55	0.57	0.62	0.55	0.55	0.53	0.42	0.55	0.55	0.49	0.48	0.48	0.48	2.2	2.82
	Lu	LF200	0.01	0.06	0.05	0.06	0.07	0.08	0.06	0.06	0.06	0.1	0.08	0.09	0.09	0.08	0.09	0.07	0.08	0.08	0.07	0.07	0.07	0.07	0.32	0.43
	Total REE	…..	…..	10.78	10.18	8.71	11.77	16.08	12.31	10.92	11.28	22.02	20.67	29.7	22.78	22.3	20.56	17.7	30.99	28.56	23.81	22.78	21.52	18.77		
Ratios	LREE	…..	…..	8.96	8.51	6.91	9.74	13.53	10.37	9.07	9.32	19.15	17.87	26.67	19.94	19.61	17.8	15.53	28.13	25.65	21.33	20.41	18.93	16.37		
	HREE	…..	…..	1.82	1.67	1.8	2.03	2.55	1.94	1.85	1.96	2.87	2.8	3.03	2.84	2.69	2.76	2.17	2.86	2.91	2.48	2.37	2.59	2.3995		
	LREE / HREE	…..	…..	4.92	5.095	3.838	4.798	5.305	5.345	4.902	4.755	6.672	6.382	8.801	7.021	7.021	7.289	6.449	7.156	9.835	8.814	8.6	8.611	7.308		

5. Results and Discussion

5.1 Major Element Geochemistry

Table1 illustrates the results of geochemical analysis of the studied Gercus sandstones and computed parameters for provenance-indicative elements. The results show enrichment in Fe_2O_3, CaO and MgO in most samples and depletion of SiO_2, Al_2O_3, MnO, Na_2O, K_2O, TiO_2 and P_2O_5 compared to Upper continental crust [6]. Relative to the average of Post-Archean Australian Shale (PAAS) [6], the sandstone samples are enriched in CaO, MgO and LOI and depleted in SiO_2, Al_2O_3, Fe_2O_3, MnO, Na_2O, K_2O, TiO_2 and P_2O_5 (Table 1 and Figure 2). The weathering condition in the source area contributes to the simultaneous reduction in elemental concentrations.

Sandstone geochemistry reflects the mineral composition of sandstones and the diagenesis process that influences sediments during the lithification process [31]. In this study, the high CaO value may be attributed to rich carbonate (i.e. calcite) content as cement material; this was confirmed by the significant positive correlation between CaO and LOI (r = 0.86; n=20); and Sr (r = 0.62; n=20).

The high concentrations of MgO and significant positive correlation between MgO and Fe_2O_3 (r = 0.73; n=20); and slight enrichment in Fe_2O_3 (wt %) content may be ascribed to the mafic source rock. The studied samples are predominantly ferromagnesian potassic sandstones with lower amounts of SiO_2, Al_2O_3, MnO, Na_2O, K_2O, TiO_2 and P_2O_5 concentrations than the UCC and PAAS, which might be connected to the chemical weathering under oxidizing conditions and / or to the chemical composition of the parent rocks.

Alkalis and alkaline earth elements were decreased during weathering processes due to the chemical degradation of rocks [31]. K_2O/Na_2O is also affected by the low and irregular amounts of Na_2O (0.98 – 25,00). Sandstone samples from the Gercus Formation often exhibit K_2O/Na_2O ratios > 1 (Please refer to Table 1 for oxide averages).

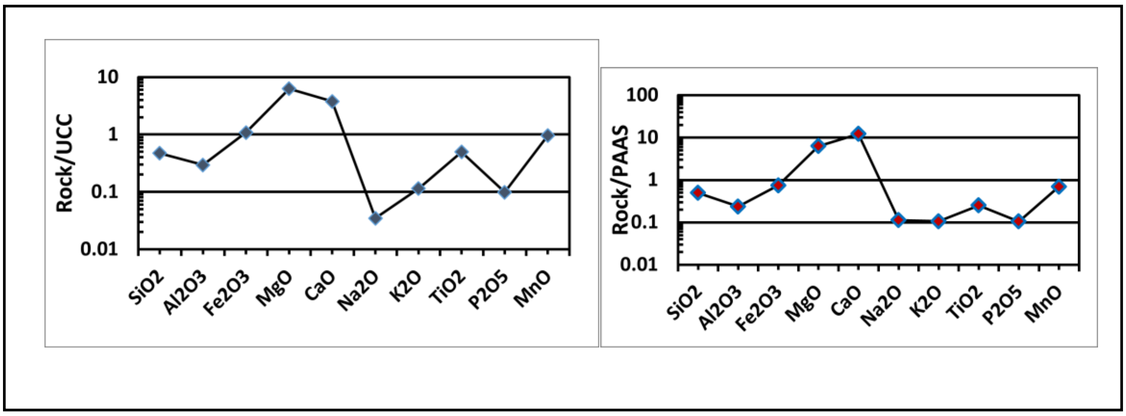

Figure 2-Major element concentrations of sandstones normalized against UCC and PAAS [6].

Various geochemical classification diagrams were utilized [30-34]. The studied sandstones samples are primarily Fe and lithic arenite with minor arkose sandstones as seen in the geochemical classification diagrams suggested by [30, 32, 34] (Figure 3a-c).
Using the chemical classification given by Pettijohn et al. [32], the examined materials were categorised as being litharenites with minor arkose (Figure 3-b). As a result, the SiO_2/Al_2O_3 ratio indicates the relative quantity of quartz and clays generated from feldspar. Major oxide discrimination [35-37] reveals that the Gercus Formation sandstone was primarily derived from quartzite, with little igneous sources (Figure 3 d). It is also clear from the ternary diagram proposed by Blatt et al. [33] that the studied samples are primarily ferromagnesian potassic sandstones (Figure 4).

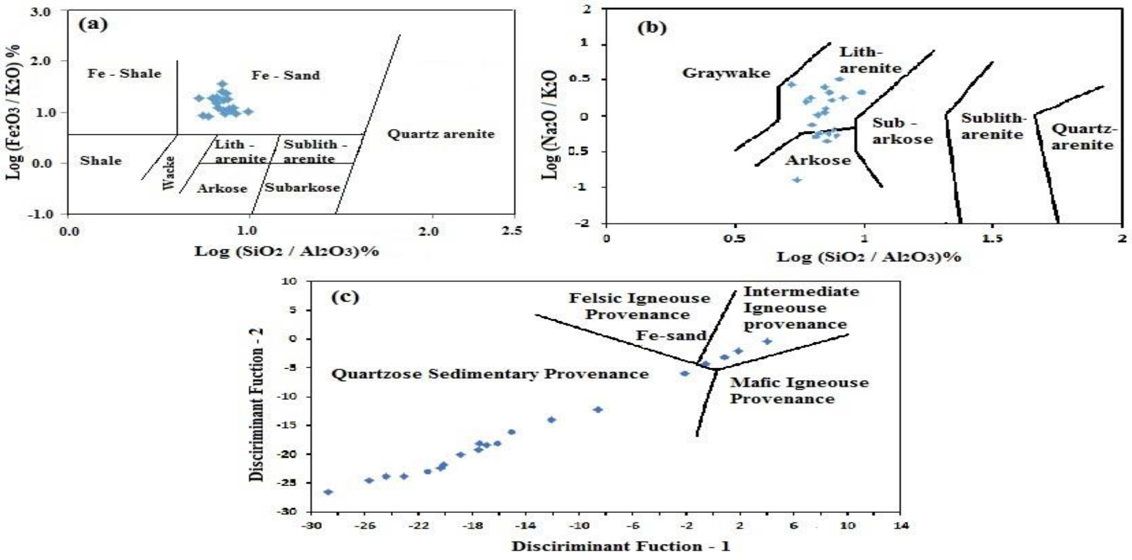

Figure 3-Geochemical classification of terrigenous sandstones using (a) log (Fe_2O_3/K_2O) versus log (SiO_2/Al_2O_3) [34]; (b) log (Na_2O/K_2O) versus log (SiO_2/Al_2O_3) [32]; and (c) Discriminant function diagram using major elements for the provenance signatures of the

sandstones [37]. Please notice that four samples are showing uncertainty within the intermediate igneous field. The discriminant functions are: Discriminant Function-1 = (−1.773 TiO_2) + (0.607 Al_2O_3) + (0.760 Fe_2O_3) + (−1.500 MgO) + (0.616 CaO) + (0.509 Na_2O) + (−1.224 K_2O) + (−9.090); Discriminant Function -2 = (0.445 TiO_2) + (0.070 Al_2O_3) + (−0.25 Fe_2O_3) + (−1.142 MgO) + (0.438 CaO) + (1.475 Na_2O) + (1.426 K_2O) + (−6.861).

5.2 Trace Element Geochemistry

Numerous variables impacted the behaviour of trace elements during sedimentary processes, including physical sorting, weathering, adsorption, diagenesis, provenance, and metamorphism [6, 36]. The Gercus sandstones (Table 1) have lower trace element concentrations than the average upper continental crust (UCC) and Post Archean Australian Shale (PAAS) concentrations except for Ni, Cr and Co and Ni, Cr, Co and Nb, respectively (Figure 5).

It has been shown that large ion lithophile elements (LILE) such as Ba, Sr, Rb, Th and U are significantly reduced in the investigated sandstone samples compared to UCC and PAAS in general. Due to their great solubility in water, these elements are highly mobile during weathering processes [31]. Since they are non-conservative elements, they can adsorb on the surface of clay minerals. Rb, Th and U contents are positively correlated with both TiO_2 (r = 0.79, 0.78 and 0.64, respectively; n=20) and P_2O_5 (r = 0.75, 0.83 and 0.63, respectively; n= 20), whereas the Ba is positively associated with SiO_2, Al_2O_3, Na_2O and K_2O (r = 0.40, 0.67, 0.31 and 0.51, respectively; n =20) (Table 1).

The High field strength elements (HFSE) like Hf, Zr, Nb, Ta and Y are dropped significantly in the investigated samples compared to UCC and PAAS, whereas Niobium (Nb) is somewhat enriched compared to PAAS. There is also favourable correlation between the HFSEs (Hf, Zr, Nb, Ta and Y) with P_2O_5 (r = 0.77, 0.84, 0.86, 0.88 and 0.56, respectively; n=20) and TiO_2 (r = 0.82, 0.85, 0.86, 0.86 and 0.57, respectively; n=20) of the investigated sandstone samples (Table 1).

The transition trace elements (TTE) in the Gercus sandstone samples are markedly enriched in Ni, Cr and Co, whereas Sc and V elements are marginally enriched. In the course of igneous fractionation, Co, Cr and Ni are compatible elements and are typically enriched in mafic to ultra-mafic rocks, whereas depleted in felsic rocks [31].

The TTEs, Co, Ni and Sc in the sandstone samples are positively correlated with SiO_2 (r = 0.92, 0.83 and 0.65, respectively; n = 20), Al_2O_3 (r = 0.75, 0.68 and 0.80, respectively; n=20), Fe_2O_3 (r = 0.71, 0.91 and 0.85, respectively; n = 20), MgO (r = 0.86, 0.87 and 0.70, respectively; n = 20) and Na_2O (r = 0.77, 0.62 and 0.31, respectively; n= 20). On the other hand, Cr is positively correlated with Fe_2O_3 and MgO (r = 0.60, 0.50, respectively; n = 20). The Cr/Th and Th/Co ratios in the sandstone samples examined range from 429 to 27000 and 0.001 to 0.026, respectively (Table1).

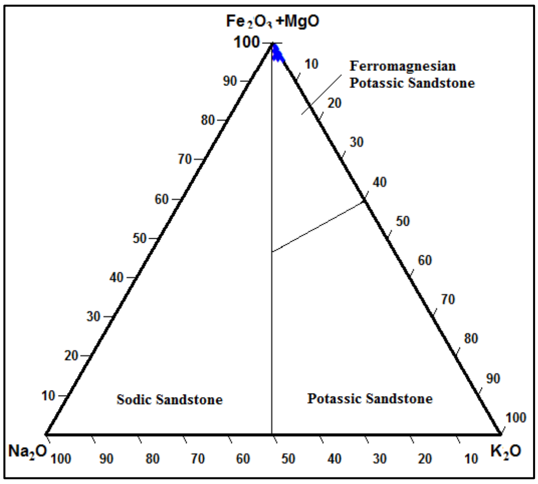

Figure 4-Ternary diagram of Na_2O-K_2O-(Fe_2O_3+MgO) of the Gercus sandstone [33].

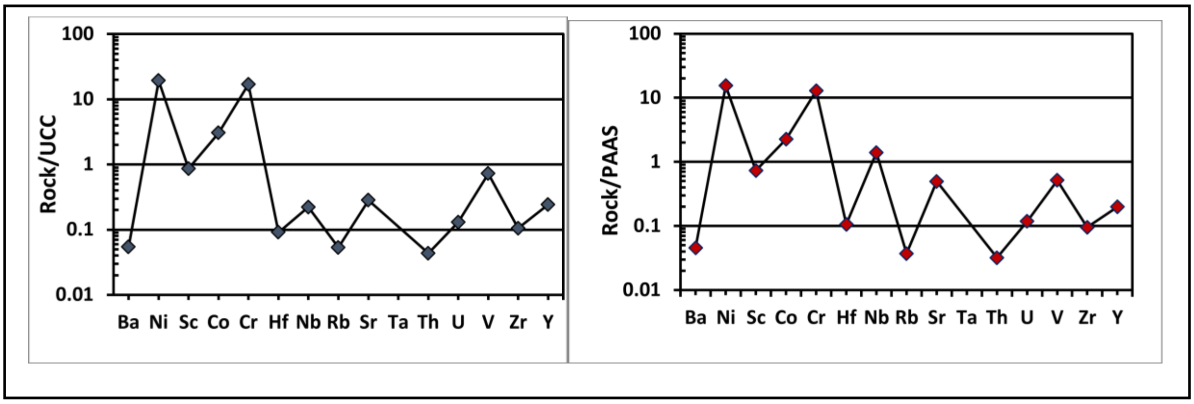

Figure 5-Trace element concentrations of sandstones normalized against UCC and PAAS [6].

5.3 Rare Earth Elements Geochemistry

Table 1 shows the relative abundances and ratios of rare earth elements (REE) in the sandstone samples examined. In comparison to UCC and PAAS, the average concentrations of incompatible light rare earth elements (LREE) and heavy rare earth elements (HREE) in sandstone samples from the Gercus Formation are decreased in La, Ce, Pr, Nd, Sm, Eu, and Gd and Tb, Dy, Ho, Er, Th, Yb, and Lu, respectively (Figure 6).

The contents of ∑REE on average in the studied sandstone is 18.771 ppm, and their enrichment factor (∑LREE / ∑HREE) ratios are 6.60 against 146.37 ppm and 184.77 ppm 13.51 and 13.27 of UCC and PASS respectively.

These findings indicate that the total REE concentration of the investigated Gercus sandstone is significantly lower than that of UCC and PAAS. The REEs have demonstrated a strong favourable relationship with CaO, TiO_2, P_2O_5 and LOI (vary from r = 0.42 to 0.89; n=20).

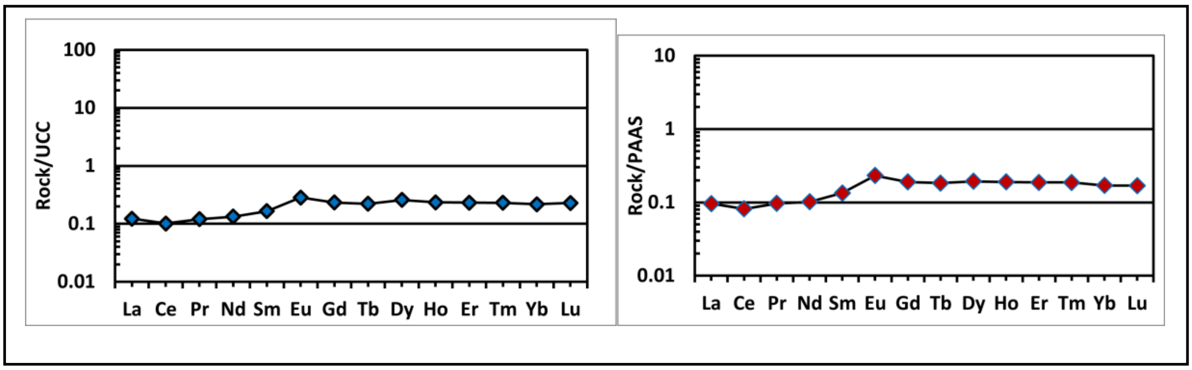

Figure 6-Rare earth concentrations of sandstones normalized against UCC and PAAS [6].

6. Provenance and Tectonic Setting

The valuable information about the clastic sediment’s provenance can be obtained from their geochemical composition [39]. The chemical composition of the siliciclastic sedimentary rocks is influenced mainly by their provenance and plate tectonic setting. This is documented by several authors [4, 33, 35, 38], and several classifications have been proposed to differentiate the various source and tectonic settings of terrigenous sedimentary rocks. Unstandardized discriminant function 3 and 4 scores of sandstone samples for the Al_2O_3 were displayed following the boundaries of provenance fields, namely, quartzose sedimentary, mafic igneous, intermediate igneous, and felsic igneous [41] (Figure 7). The studied sandstones of the Gercus Formation represent a quartzose recycled mature polycyclic detritus sediment. This could present mature continental provenance derived from a highly weathered granite gneiss or sedimentary terrane, where Kettanah et al [7] indicated that the sedimentary provenance for most sandstones and mudstones in the Middle Eocene the Gercus Formation are quartz and less intermediate igneous provenance.

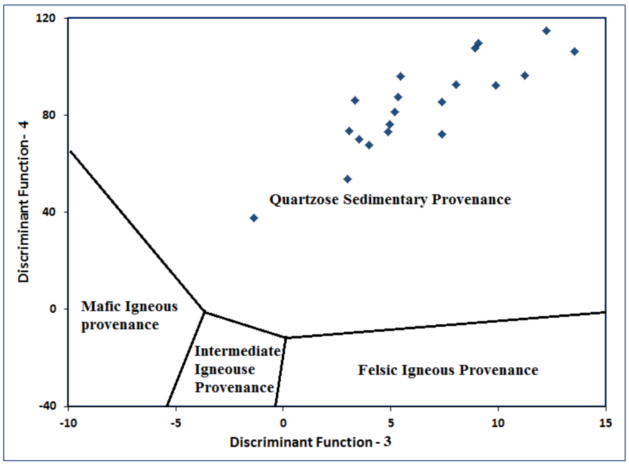

Figure 7 -Discriminant function diagram using major elements for the provenance signatures of the sandstones after [37-41]. The discriminant functions are: Discriminant Function-3 = (30.638 TiO_2/Al_2O_3) - (12.541 Fe2O3/ Al_2O_3) + (7.329 MgO/ Al_2O_3) + (12.030Na2O/ Al_2O_3) + (35.400 K2O/ Al_2O_3) - (6.382); Discriminant Function -4 = (56.500 TiO_2/ Al_2O_3) - (10.879 Fe2O3/ Al_2O_3) + (30.875MgO/ Al_2O_3) - (5.404 Na2O/ Al_2O_3) + (11.110 K2O/ Al_2O_3) - (3.890).

The ternary plot employed by Englund and Jørgensen [42], which is based on major oxides (i.e. Al_2O_3, K_2O+Na_2O+CaO and Fe_2O_3+MgO), was used to illustrate the depositional affinity of the studied Gercus Formation as shown in Figure 8.

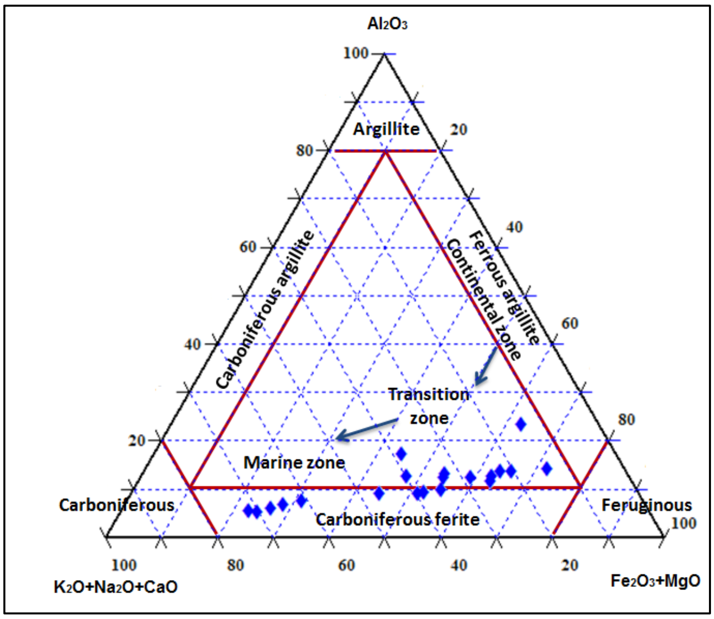

Figure 8-Al_2O_3 – (K_2O+Na_2O+CaO) and (Fe_2O_3+MgO) ternary diagram for the environmental deposition of the Gercus Formation (after [42]).

Certain trace elements such as HFSEs, LILEs and some TTEs are used to determine the provenance due to their low mobility nature [40]. Moreover, high-field-strength elements (HFSE) such as Zr, Nb, Hf, Y, and Th are concentrated in felsic magma's crystallisation process [6]. Because of their low mobility throughout sedimentation and short residence periods in seawater, REE and Sc can provide information about source compositions [4].

In the opinion of Dokuz and Tanyolu [43], the trace elements (Th and Sc) are used to confirm the provenance of studied rock samples (Figure 9-a). The Sc is a compatible element enriched in mafic rocks, while Th is an incompatible element enriched in felsic rocks. The Th/Sc ratio = 1.0 reflect a typical continental crust source rich with incompatible elements as a result of chemical differentiation that depends on sediment recycling [1], whilst the Th/Sc ratio equal to 0.60, is usually a mafic source enriched in Sc element [44]**,** as in the studied the Gercus Formation.

The ratios of compatible and incompatible elements, such as Zr/Sc and Th/Sc, clearly identify the difference between mafic and felsic sources, sorting processes, sediment recycling [1], heavy mineral assemblage, and compositional maturity [45]. The relationship between the source rock composition and sedimentary processes on the composition of clastic sedimentary rocks is identified by Zr/Sc versus Th/Sc plot [1] (Figure 9-b).

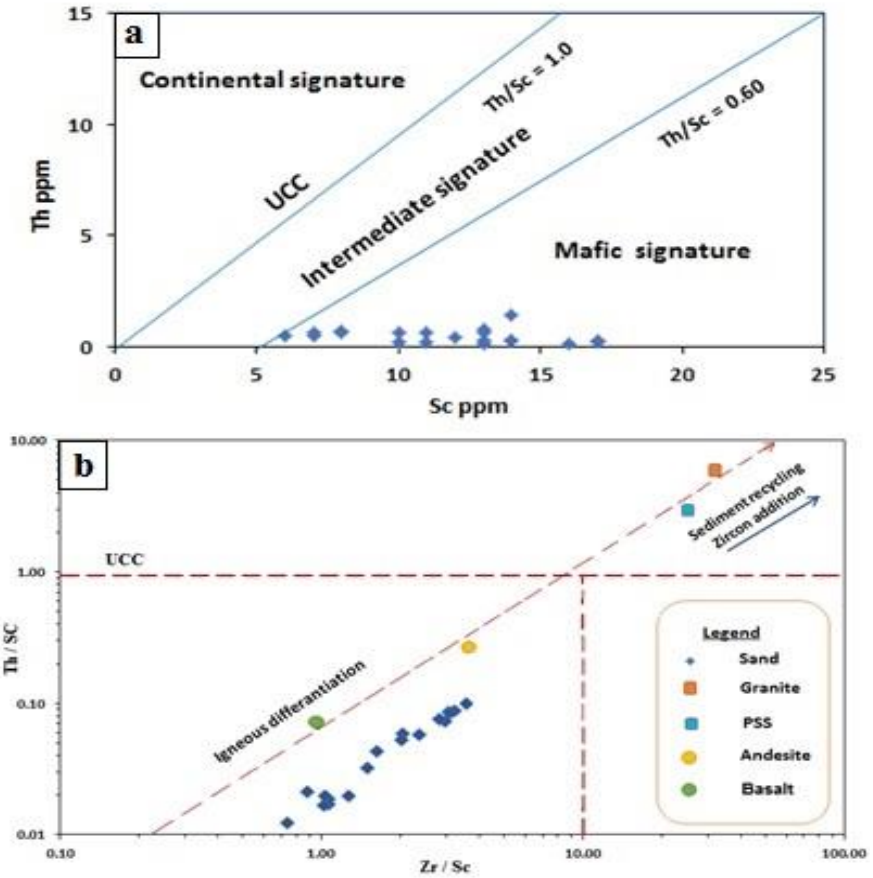

Figure 9-(a) Provenance discrimination diagram for the sandstones of the Gercus Formation (after [43]). (b) Zr/Sc versus Th/Sc diagram for the Gercus Formation sandstones (after [1]).

This plot reveals that the Gercus sandstone samples concentrated near the basalt and andesite are located under the upper continental crust field, which indicates the provenance of the Gercus Formation sandstone is originated from basalt and mixed with andesite as a minor. The La/Th versus Hf discrimination diagram of Floyd and Leveridge [46] indicates that the studied siliciclastic rocks are of andesitic arc source rocks origin with lower continental crust (LLC) influence [1]; (Figure 10-a). Furthermore, the significant positive correlation between TiO_2 and Zr (r = 0.85; n=20) in this study highlights the concentration of certain accessory minerals such as rutile, zircon, and ilmenite [1]. Moreover, the plot of Zr versus TiO_2 (Figure 10-b) resembles mafic, intermediate, and felsic igneous rocks provenance [47] and thus reflect mafic igneous rocks influence.

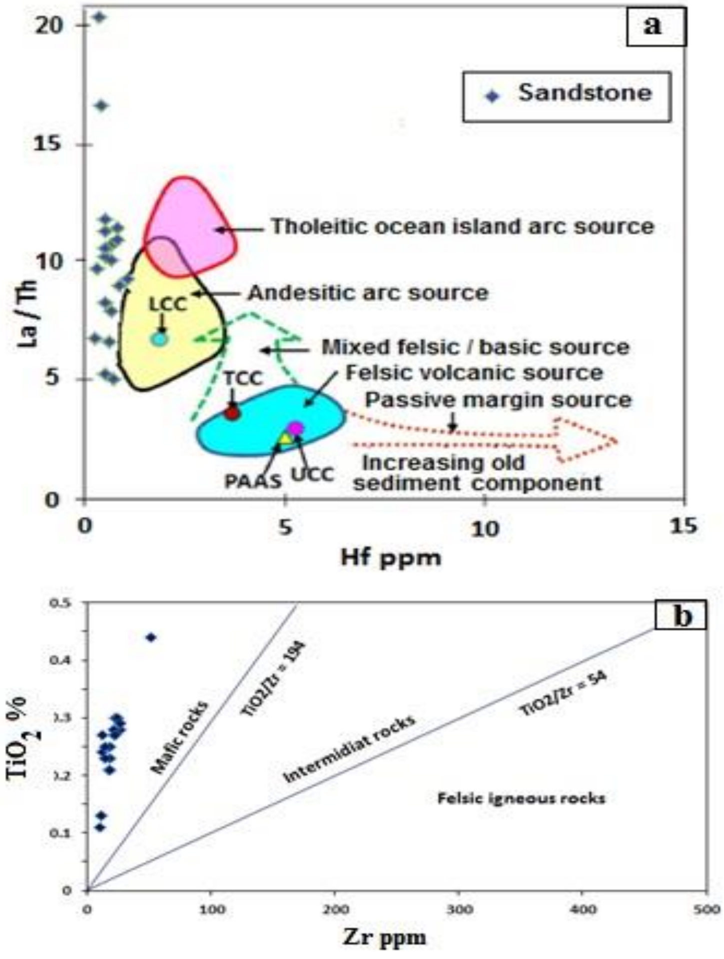

Figure 10-(a) La /Th versus Hf source and a compositional diagram for the Gercus Formation sandstones (after [46]), (b) TiO_2 versus Zr diagram for the Gercus Formation sandstones (after [47]).

The chemical composition of sandstone is implemented by several workers (e.g. [4, 33, 35, 38, 46]) to understand the tectonic setting of the source area. On the discrimination diagram suggested by Roser and Korsch [35] plotting SiO_2 *versus* log (K_2O/Na_2O) of clastic sediments, the Gercus sandstone samples demonstrate oceanic island arc margin origin (Figure 11).

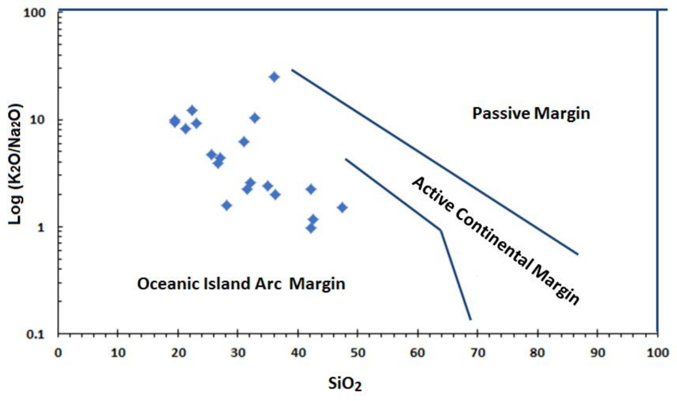

Figure 11-Tectonic discrimination diagram for the clast sediments of the Gercus Formation (adopted by [35]).

Based on Bhatia [40], the relationship between major oxides Fe_2O_3+MgO with TiO_2 (Figure 12-a) and Al_2O_3/ SiO_2 ratio (Figure 12-b) were used to distinguish the tectonic setting of a source area. These trends of mafic elements between Fe_2O_3+MgO along with TiO_2 and with the Al_2O_3/ SiO_2 ratio provide oceanic island arc and minimal influence of active continental margin with mafic enrichments of the Gercus Formation source rocks (Figure 12- a, b) .

Furthermore, the comparison of Fe_2O_3+MgO contrastwith the Al_2O_3/SiO_2 ratio demonstrates the relatively homogeneous mafic content of the Gercus Formation source rock composition. While the depletion in Al_2O_3/ SiO_2 ratio could be linked to high SiO_2 and low Al_2O_3 content, which is impacted by the intensive weathering and sediments maturation in semi oceanic island arc setting with active continental margin influence. The high ferromagnesium components Fe_2O_3+MgO indicated a high percent in source rocks.

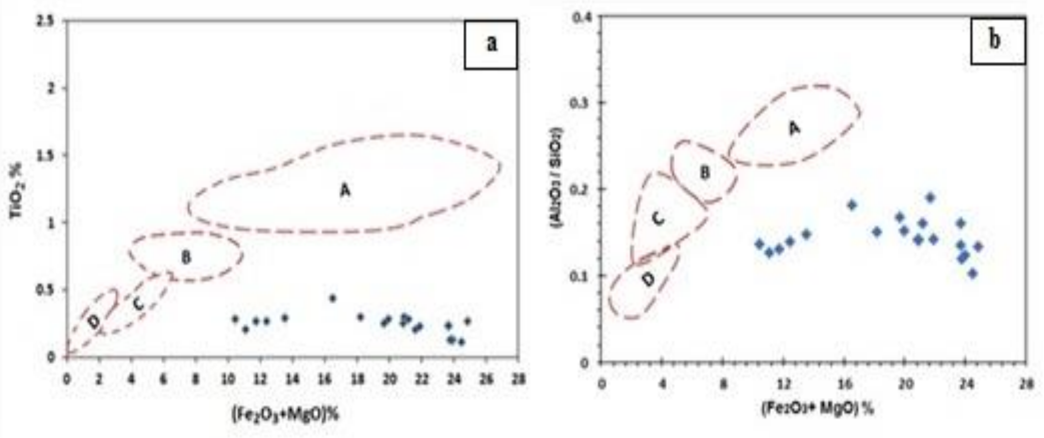

Figure 12-(a) Tectonic discrimination diagram of: a, (Fe_2O_3+MgO) % versus TiO_2 %; (b) (Fe_2O_3+MgO) % versus (Al_2O_3/SiO_2) ratio for the clast sediments of the Gercus Formation. Were A, oceanic island arc; B, continental arc; C, active continental margin; D, passive continental margin (fields after [4]).

The variations in Sc and Co (indicative of mafic) and Th and La (indicative of felsic) contents have been used to differentiate between mafic and felsic provenance by various authors [6, 47]. The La-Th-Sc triangular diagram after Bhatia and Crook [4] is also used to understand the tectonic environment (Figure 13). It is divided into four fields: oceanic island arc, continental arc, active continental margin and passive continental margin.

This diagram was divided by Sinha et al. [48,49] into three fields: felsic, intermediate, and mafic rock to discriminate the type of source rocks. The plot of sandstone samples of the Gercus Formation cluster in the A field derives the clastics from an oceanic island arc margin. Furthermore, most of the studied sandstone samples are plotted near the field 3 which meaning that clast is sourced from mafic rocks (Figure 13).

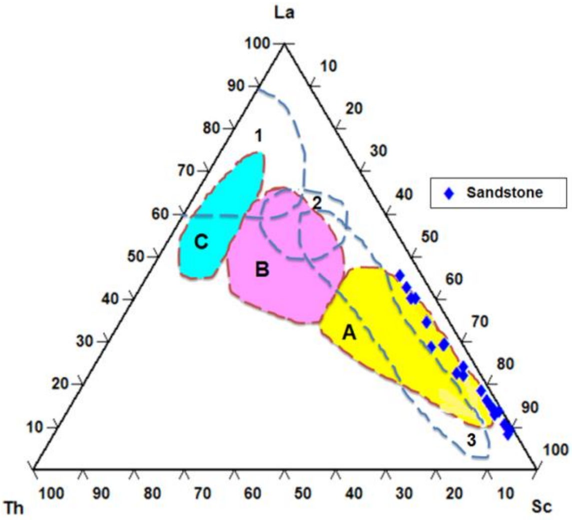

Figure 13-Th, La, Sc tectonic discrimination diagram for the sandstone of the Gercus Formation. A, oceanic island arc; B, continental arc; C, active continental margin; D, passive continental margin (fields after [4]). Field 1 is felsic, field 2 is intermediate, and field 3 is mafic rocks [49].

The Th–Co–Zr/10 and Th–Sc –Zr/10 tectonic discriminating diagrams [4] (Figure 14-a,b) for immobile trace elements in clastic sediments show most of the studied samples are found within and near the Oceanic Island Arc (OIA) margin and pointed out that the sandstone rocks of the Gercus Formation are related to the (OIA) tectonic environment.

Based on the findings, it was suggested that the Gercus Formation was deposited in an OIA tectonic setting after the initial collision between Afro-Arabian Plate with the Iranian–Eurasian Plate during the Early Cretaceous [50].

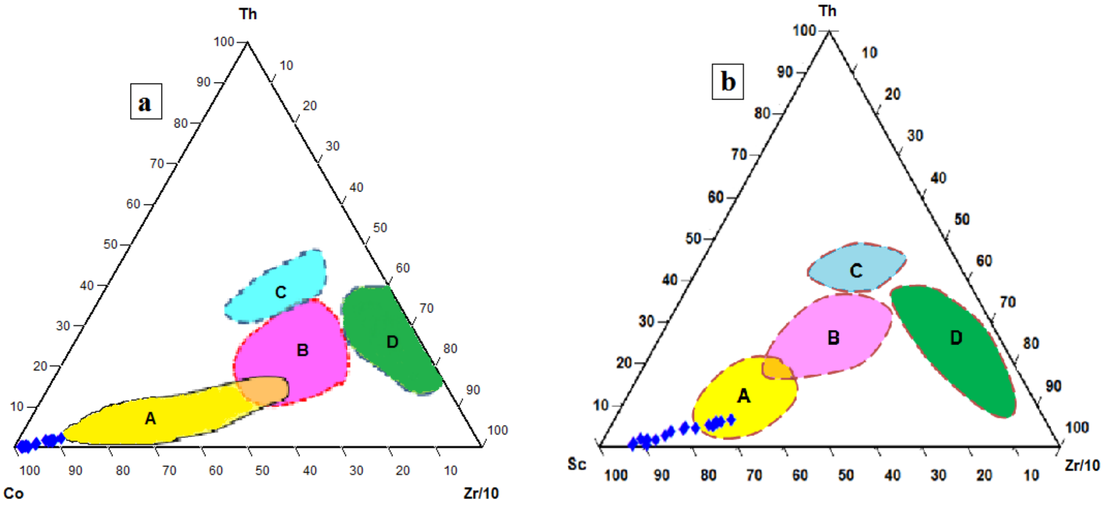

Figure 14-(a):- Th, Co, Zr/10 tectonic discrimination plot illustrates the Gercus Formation clasts as oceanic arc margin. (b):- Th, Sc, Zr/10 tectonic discrimination plot shows the Gercus Formation clasts as oceanic arc margin. Were A, oceanic island arc; B, continental arc; C, active continental margin; D, passive continental margin (fields after [4]).

7. Paleo-weathering Source area

The chemical composition of clastic sedimentary rocks is mainly determined by the parent rock's nature and weathering conditions [49, 50]. However, the geochemical composition of clastic sedimentary rocks is a valuable tool to assess the weathering processes, the geochemical composition [2] and the palaeogeography of the source area. The nature of the weathering process defines the mineral and geochemical characterisation of the sediments [51, 52]along with rock composition, tectonic setting and climatic conditions [2, 53].

The Chemical Index of Alteration (CIA) [53, 54, 55, 56], Chemical Index of Weathering (CIW) [56] and Plagioclase Index of Alteration (PIA) [57] indicates the degree of weathering and elemental redistribution in the source region, therefore they are widely used to evaluate the intensities of weathering and alteration of the source rock .

The intensity of source rock weathering is addressed in molar percentage of the oxide components calculated by the Chemical Index of Alteration (CIA = [Al_2O_3/(Al_2O_3 + CaO* + Na_2O + K_2O)]* 100) [49, 55, 56], Chemical Index of Weathering (CIW [Al_2O_3/ (Al_2O_3 + CaO_ + Na_2O)] * 100) [56] and Plagioclase Index of Alteration (PIA = [(Al_2O_3 – K_2O)/(Al_2O_3 + CaO* + Na_2O - K_2O)]* 100) [39, 55] .

Where CaO* represents Ca in siliciclastic bearing minerals and the samples with the high content of CaO is relat¬ed to the cement diagenetic and must be corrected according to the equation {CaO* = CaO - (10.3 × P_2O_5)} proposed by Fedo et al. [57]. It is assumed that CaO is equal to Na_2O if it exceeds Na2O. No adjustment is needed if it is less than Na2O [1].

The CIA is an excellent indicator of palaeoweathering conditions since it effectively tracks the weathering of feldspars to clay minerals [2, 56]. Mineral alteration proceeds in a very organized manner is extreme (CIA>80) to intermediate (CIA = 60–80) to incipient (CIA = 50–60) chemical weathering. The values of CIA of the Gercus Formation sandstone vary from 70.52 to 98.03 (average = 89.72; Table 1). These values revealed the studied sandstone were subjected to intense (extreme) chemical weathering (Table 1).

The Gercus Formation clastic sandstone data were plotted in Al_2O_3 – CaO+Na_2O – K_2O (A-CN-K) diagrams to determine the source rock's character in terms of weathering, diagenesis, and chemical composition. In this plot, the Gercus sandstones suggest that the source has undergone extensive chemical weathering (Figure 15).

As a result of the extensive chemical weathering, the source area has been subjected to warm, humid climatic conditions and a reduction in tectonic activity [38]. Smectite clay minerals dominate the majority of the samples tested. As a result, a plot of CIA against Al_2O_3 [58] indicates that the majority of the Gercus sandstone samples examined were subjected to severe weathering (Figure 16).

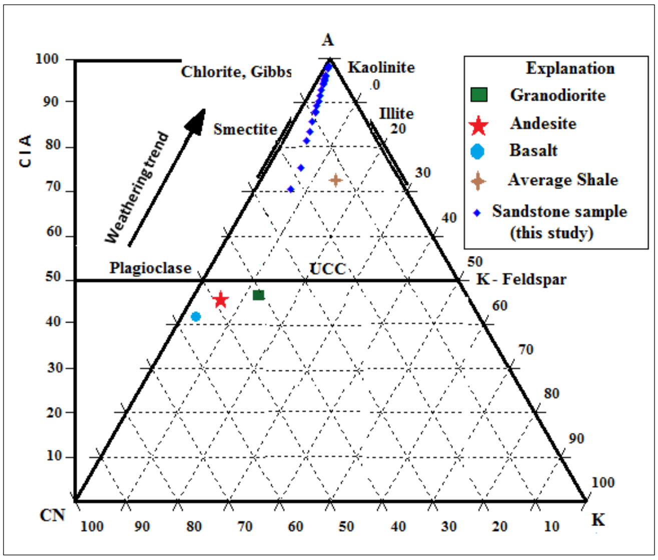

Figure 15-Al_2O_3 – CaO+Na_2O – K_2O (A-CN-K) ternary diagram for the studied the Gercus sandstone, after [54].

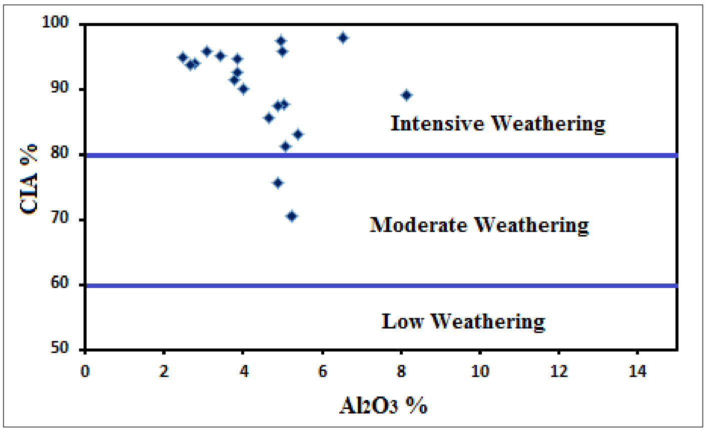

Figure 16-Scatter plot of CIA versus Al_2O_3 after [58].

In addition to the CIA, the chemical index of weathering (CIW) is employed in this study to monitor paleo-weathering in the source area and gives information on the degree of chemical weathering the sediments have undergone [41]. The CIW is the same as the CIA, and only it does not include K_2O in the calculation.

The difficulties associated with K remobilization during diagenesis and metamorphism are avoided using this index. Harnois [56] argued that the CIW excludes K since it might be leached or accumulated in the residual sediments during weathering. This index is unaffected by post-depositional potassium enrichment.

By Harnois [56], a CIW value between 0-40 refers to low weathering and 40-65 moderately weathered and > 70 intense weathered sediments. The siliciclastic sandstones of the Gercus Formation possess CIW values ranging from 76.07 to 98.52 (averaging 91.95). These high values imply that the source areas were exposed to intense chemical weathering under humid paleoclimate conditions.

The Plagioclase Index of Alteration (PIA) can be used to evaluate the degree of source area weathering and elemental redistribution during diagenesis [39, 55]. The PIA values of studied sandstones range from 74.03 to 98.51 (averaging 91.61). These high values demonstrate the extensive degradation of the parent material through weathering, transportation, sedimentation, and diagenesis and may suggest humid and/or warm climatic conditions [59]. The cumulative influence of numerous cycles of sedimentary recycling, humid climate, higher temperature, and more extended chemical weathering of the Gercus Formation is shown by the higher CIA, CIW, and PIA [60].

8. Maturity and Paleoclimate

Because it is susceptible to weathering and sediment recycling, the SiO_2/Al_2O_3 ratios of siliciclastic rocks are widely employed as an indicator of sedimentary maturation [31]. In sandstones, the value of this ratio > 5.0 indicated increasing maturity [31]. The Gercus sandstone's SiO_2/Al_2O_3 ratios range from 5.3 to 9.75, with an average of 7.075. Suttner and Dutta [61] used the K_2O/Al_2O_3 ratio and bivariate plot SiO2 vs Al2O3+K2O+Na2O to determine the compositional maturity of the investigated sandstone (Figure 17).

The ratios $K_2O/Al_2O_3 < 0.4$ in ancient fine-grained sediments, as reported by Cox et al. [62]**,** represents low alkali feldspar abundance relative to other minerals in the original siliciclastic rocks. As a result, the average ratio of the investigated samples is $K_2O/Al_2O_3 = 0.091$, indicating a low feldspar concentration. Furthermore, the low K_2O/Al_2O_3 ratio in the examined sandstone samples might be due to the source area's predominance of low-grade metamorphic and sedimentary rocks, which typically have low feldspar abundance [63].

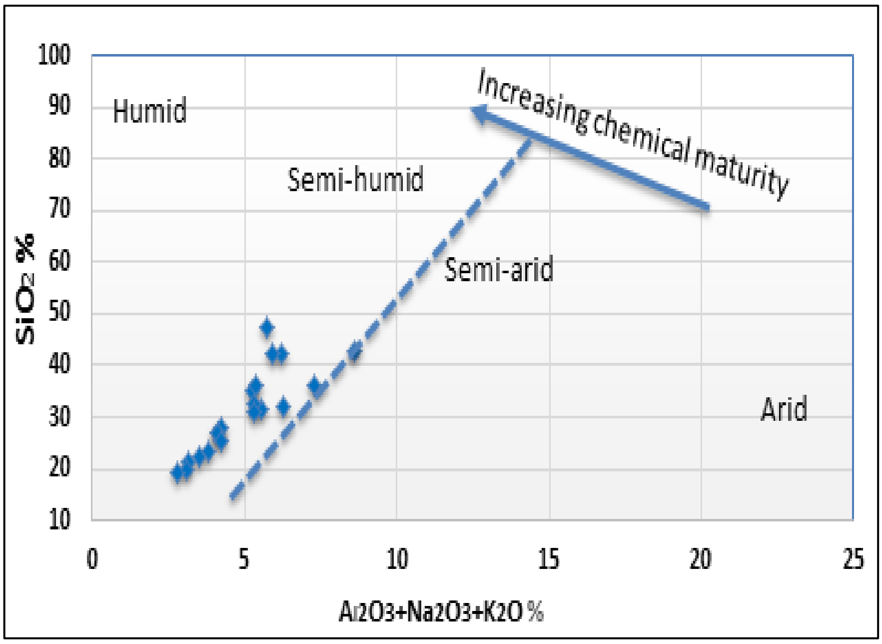

Figure 17-shows the chemical maturity of sandstone samples from the Gercus Formation (after [61]).

It is clear from the SiO_2 against Al_2O_3+K_2O+Na_2O plot diagram that the examined sandstone samples are located in humid and semi-humid areas, which indicates that humid climatic conditions prevailed during deposition of the studied sandstone samples. Chemical weathering of bedrock is typically linked with humid and warm temperature conditions, whereas comparatively moderate chemical weathering is associated with more dry climate conditions [38].

By degrading parent rocks, the climate influences sand composition. The leaching of more mobile elements is more evident in a hot and humid climate than for more stable elements [61], as a result, the CIA values in the sediments are higher. Because the examined Gercus sandstone has high CIA values, the source rocks were subjected to significant chemical weathering and developed under warm and humid climatic conditions.

9. Conclusion

The conclusions of this study can be summarized by the following:

1- The studied sandstone is classified as litharenites with minor arkose.

2- The studied samples show depletion in major and trace elements contents, except for CaO, MgO and Ni, Co, Cr respectively, when compared to the average UCC and PAAS. While all REEs revealed general depletion when compared to UCC and PAAS contents.

3- The clasts in the Gercus Formation are originated from basalt and andesite as a minor constituent with influence from the lower continental crust.

4- The Gercus Formation rocks show an influence of the OIA tectonic setting and the limitation of the active continental edge.

5- The studied sandstones indicates that it has undergone extensive chemical weathering and has formed under warm and humid climatic conditions.

References

[1] S. M. McLennan, S. Hemming, D. K. McDaniel, and G. N. Hanson, “Geochemical approaches to sedimentation, provenance, and tectonics,” *Special Papers-Geological Society of America*, p. 21, 1993.

[2] J. S. Armstrong-Altrin, Y. il Lee, S. P. Verma, and S. Ramasamy, “Geochemistry of sandstones from the upper Miocene Kudankulam Formation, southern India: Implications for provenance, weathering, and tectonic setting," *Journal of sedimentary Research*, vol. 74, no. 2, pp. 285–297, 2004.

[3] M. A. Ramos-Vázquez and J. S. Armstrong-Altrin, "Provenance and palaeoenvironmental significance of microtextures in quartz and zircon grains from the Paseo del Mar and Bosque beaches, Gulf of Mexico," *Journal of Earth System Science*, vol. 129, no. 1, pp. 1–16, 2020.

[4] M. R. Bhatia and K. A. W. Crook, "Trace element characteristics of graywackes and tectonic setting discrimination of sedimentary basins," *Contributions to mineralogy and petrology*, vol. 92, no. 2, pp. 181–193, 1986.

[5] S. M. Mclennan, "Rare earth elements in sedimentary rocks: influence of provenance and sedimentary processes," *Geochemistry and mineralogy of rare earth elements*, pp. 169–200, 1989.

[6] S. R. Taylor and S. M. McLennan, "The continental crust : its composition and evolution : an examination of the geochemical record preserved in sedimentary rocks." Blackwell Scientific, Oxford : 1985.

[7] Y. A. Kettanah, J. S. Armstrong-Altrin, and F. A. Mohammad, "Petrography and geochemistry of siliciclastic rocks of the Middle Eocene Gercus Formation, northern Iraq: Implications for provenance and tectonic setting," *Geological Journal*, vol. 56, no. 5, pp. 2528–2549, 2021.

[8] T. Buday, "The Regional Geology of Iraq. Vol. 1. Stratigraphy and Paleogeography," *Som, b. Baghdad, Dar El-Kutib Publ. House, Univ. of Mosul., p. p445*, 1980.

[9] V. K. Sissakian and B. S. Al-Jiburi, "Stratigraphy of the high folded zone," Iraqi Bulletin of Geology and Mining, vol. Special Issue, no. 6, pp. 73–161, 2014.

[10] S. Z. A. K. Al-Mashaikie, A. T. A. Al-Azzawi, and A. K. Kadhum, "Lithofacies Architecture of the Gercus Formation in Jabal Haibat Sultan, NE Iraq; New Concept of Lithostratigraphy and Depositional Environmental," *Journal of Environment and Earth Science*, vol. 3, no. 12, pp. 97–114, 2013.

[11] S. Z. A. K. Al-Mashaikie, A. T. A. Al-Azzawi, and A. K. Kadum, "Depositional Environment of the Gercus Formation in Jabal Haibat Sultan, NE Iraq; New Sedimentological Approach," *Iraqi Journal of Science*, vol. 55, no. 2A, pp. 471–483, 2014.

[12] B. Al-Qayim, S. Al-Shaibani, and B. Nissan, "A bimodal tidal depositional system of the Gercus Formation, Shaqlawa area, Northern Iraq," *Iraqi Geological Journal*, vol. 27, no. 2, pp. 75–95, 1994.

[13] Y. Al-Rawi, "Petrology and sedimentology of the Gercus red beds Formation (Eocene), Northeastern Iraq," *Iraq Journal of Science*, vol. 21, pp. 132–188, 1980.

[14] Y. Al-Rawi, "Origin of red color in the Gercus Formation (Eocene), northeastern Iraq," *Sedimentary Geology*, vol. 35, no. 3, pp. 177–192, 1983.

[15] B. M. Ameen, "Sedimentological study Gercus Formation in Northeast Iraq," *Unpubl. M. Sc. Thesis*, University of Baghdad. 103 p. 1998.

[16] K. H. Awad and H. A. A. Alsultan, "Stratigraphic Analysis of Gercus Formation in Dohuk area, Northern Iraq," *Iraqi Journal of Science*, pp. 2293–2302, 2020.

[17] M. M. Q. Baziany, "Geology of bedded Gypsum in the Gercus Formation (Early-Middle Eocene) in Dohuk area, Kurdistan Region, Northern Iraq," in *The Proceedings of third International Conferences on Geo-Resources of the Middle East and North Africa (GRMENA-III), Egypt, Cairo University*, 2009, vol. 1.

[18] S. H. Hussain and T. A. Aghwan, "Sedimentology and evolution of a foreland desert basin, Middle Eocene Gercus Formation (North and Northeastern Iraq)," *Arabian Journal of Geosciences*, vol. 8, no. 5, pp. 2799–2830, 2015.

[19] S. Z. Jassim and J. C. Goff, "Phanerozoic development of the northern Arabian Plate," in geology of Iraq, S.Z. Jassim and J.C. Goff, Eds. Dolin, Prague, pp. 32–44, 2006.

[20] Y. A. Kettanah and A. H. Bamarni, "Petrogenesis, geochemistry, and tectonic setting of a basaltic body within the Gercus Formation of northern Iraq: first record for Eocene anorogenic volcanic activity in the region," *Turkish Journal of Earth Sciences*, vol. 27, no. 6, pp. 460–491, 2018.

[21] R. C. van Bellen, H. v Dunnington, R. . Wetzel, and D. M. Morton, *Lexique Stratigraphique International: Asie. Iraq. Tertiary. Mesozoic and Palaeozoic*. Centre National de la Recherche Scientifique, 1959.

[22] T. K. Al-Ameri, A. S. Al-Dulaimy, Y. K. Ibrahim, and B. M. Amin, “Age evaluation of Gercus Formation using stratigraphic ranges of identified palynomorphs northern Iraq,” *Jo. Geol. Soc. Iraq*, 2004.

[23] B. Al-Qayim and B. Nisan, “Sedimentary Facies Analysis of A Paleogene Mixed Carbonate-Clastic Sequence, Haibat-Sultan Ridge, Northeast Iraq,” Iraqi Journal of Science, vol. 30, no. 4, 1989.

[24] Z. D. Al-Shaikh, S. A. Saleh, and H. F. Abdo, “Contribution to the Geology of Shqlawa-Harir Area Iraq,” *Jour. Geol. Soc. Special Issue*, 1975.

[25] B. Al-Qayim and L. Salman, “Lithofacies Analysis of Kolosh Formation, Shaqlawa Area, North Iraq,” *Journal of the Geological Society of Iraq*, vol. 19, no. 3, pp. 107–117, 1986.

[26] A. M. Surdashi Lawa F.A., “Stratigraphy, Microfacies and Depositional Environment of Sinjar Formation in Studied Section, NE. Iraq,” in *Proceedings of 2nd Scientific Conference of the University of Salahaddin-Erbil*, 1993, no. Special Issue, pp. 77–110.

[27] F. A. Lawa, “Sequence stratigraphic analysis of the Middle Paleocene–Middle Eocene in the Sulaimani district (Kurdistan region),” *Unpublished Ph. D. thesis, University of Sulaimani*, 2004.

[28] H. Y. Dhannoun, S. M. A. Al-Dabbagh, and A. A. Hasso, “The geochemistry of the Gercus red bed formation of northeast Iraq,” *Chemical Geology*, vol. 69, no. 1–2, pp. 87–93, 1988.

[29] A. I. Al-Juboury, S. H. Hussain, T. McCann, and T. A. Aghwan, “Clay mineral diagenesis and red bed colouration: A SEM study of the Gercus Formation (Middle Eocene), northern Iraq,” *Geological Journal*, vol. 55, no. 12, pp. 7977–7997, 2020.

[30] R. A. Abdula and R. N. S. Khailany, “Shiranish Formation in Garota (Shaqlawa, North Iraq) as raw material for portland cement manufacturing,” *Iraqi Bulletin of Geology and Mining*, vol. 12, no. 1, pp. 65–72, 2016.

[31] B. P. Roser, R. A. Cooper, S. Nathan, and A. J. Tulloch, “Reconnaissance sandstone geochemistry, provenance, and tectonic setting of the lower Paleozoic terranes of the West Coast and Nelson, New Zealand,” *New Zealand Journal of Geology and Geophysics*, vol. 39, no. 1, pp. 1–16, 1996.

[32] F. J. Pettijohn, P. E. Potter, and R. Siever, *Sand and sandstone*. Springer Science & Business Media, 2012.

[33] H. Blatt, G. v Middleton, and R. C. Murray, Origin of sedimentary rocks. Prentice-Hall, Inc., 1972.

[34] M. M. Herron, “Geochemical classification of terrigenous sands and shales from core or log data,” *Journal of sedimentary Research*, vol. 58, no. 5, pp. 820–829, 1988.

[35] B. P. Roser and R. J. Korsch, “Determination of tectonic setting of sandstone-mudstone suites using SiO2 content and K2O/Na2O ratio,” *The Journal of Geology*, vol. 94, no. 5, pp. 635–650, 1986.

[36] D. A. Lindsey, “An evaluation of alternative chemical classifications of sandstones,” US Geological Survey, Denver, Open File, Report 99–346, 1999.

[37] B. P. Roser and R. J. Korsch, “Provenance signatures of sandstone-mudstone suites determined using discriminant function analysis of major-element data,” *Chemical Geology*, vol. 67, no. 1–2, pp. 119–139, 1988.

[38] Hw. Nesbitt and G. M. Young, “Early Proterozoic climates and plate motions inferred from major element chemistry of lutites,” *nature*, vol. 299, no. 5885, pp. 715–717, 1982.

[39] J. S. Armstrong-Altrin, Y. il Lee, J. J. Kasper-Zubillaga, and E. Trejo-Ramírez, “Mineralogy and geochemistry of sands along the Manzanillo and El Carrizal beach areas, southern Mexico: implications for palaeoweathering, provenance and tectonic setting,” *Geological Journal*, vol. 52, no. 4, pp. 559–582, 2017.

[40] M. R. Bhatia, “Plate tectonics and geochemical composition of sandstones,” *The Journal of Geology*, vol. 91, no. 6, pp. 611–627, 1983.

[41] C. Baiyegunhi, K. Liu, and O. Gwavava, “Geochemistry of sandstones and shales from the Ecca Group, Karoo Supergroup, in the Eastern Cape Province of South Africa: Implications for provenance, weathering and tectonic setting,” *Open Geosciences*, vol. 9, no. 1, pp. 340–360, 2017.

[42] J.O. Englund and P. Jørgensen, "A chemical classification system for argillaceous sediments and factors affecting their composition," *Geologiska Föreningen i Stockholm Förhandlingar*, vol. 95, no. 1, pp. 87–97, 1973.

[43] A. Dokuz and E. Tanyolu, "Geochemical constraints on the provenance, mineral sorting and subaerial weathering of Lower Jurassic and Upper Cretaceous clastic rocks of the eastern Pontides, Yusufeli (Artvin), NE Turkey," *Turkish Journal of Earth Sciences*, vol. 15, no. 2, pp. 181–209, 2006.

[44] M. W. Totten, M. A. Hanan, and B. L. Weaver, "Beyond whole-rock geochemistry of shales: the importance of assessing mineralogic controls for revealing tectonic discriminants of multiple sediment sources for the Ouachita Mountain flysch deposits," *Geological Society of America Bulletin*, vol. 112, no. 7, pp. 1012–1022, 2000.

[45] J. S. Armstrong-Altrin, M. L. Machain-Castillo, L. Rosales-Hoz, A. Carranza-Edwards, J.-A. Sanchez-Cabeza, and A. C. Ruíz-Fernández, "Provenance and depositional history of continental slope sediments in the Southwestern Gulf of Mexico unraveled by geochemical analysis," *Continental Shelf Research*, vol. 95, pp. 15–26, 2015.

[46] P. A. Floyd and B. E. Leveridge, "Tectonic environment of the Devonian Gramscatho basin, south Cornwall: framework mode and geochemical evidence from turbiditic sandstones," *Journal of the Geological Society*, vol. 144, no. 4, pp. 531–542, 1987.

[47] K.-I. Hayashi, H. Fujisawa, H. D. Holland, and H. Ohmoto, "Geochemistry of∼ 1.9 Ga sedimentary rocks from northeastern Labrador, Canada," *Geochimica et Cosmochimica Acta*, vol. 61, no. 19, pp. 4115–4137, 1997.

[48] S. M. McLennan, S. R. Taylor, M. T. McCulloch, and J. B. Maynard, "Geochemical and Nd-Sr isotopic composition of deep-sea turbidites: crustal evolution and plate tectonic associations," *Geochimica et Cosmochimica Acta*, vol. 54, no. 7, pp. 2015–2050, 1990.

[49] S. Sinha, R. Islam, S. K. Ghosh, R. Kumar, and S. J. Sangode, "Geochemistry of Neogene Siwalik mudstones along Punjab re-entrant, India: Implications for source-area weathering, provenance and tectonic setting," *Current Science*, pp. 1103–1113, 2007.

[50] K. W. Glennie, "Cretaceous tectonic evolution of Arabia's eastern plate margin: a tale of two oceans," SEPM (Society for Sedimentary Geology) Spec. Publ., no. 69, pp. 9–20, 2000.

[51] H. W. Nesbitt and G. M. Young, "Formation and diagenesis of weathering profiles," *The Journal of Geology*, vol. 97, no. 2, pp. 129–147, 1989.

[52] H. W. Nesbitt and G. M. Young, "Petrogenesis of sediments in the absence of chemical weathering: effects of abrasion and sorting on bulk composition and mineralogy," *Sedimentology*, vol. 43, no. 2, pp. 341–358, 1996.

[53] H. W. Nesbitt and G. M. Young, "Prediction of some weathering trends of plutonic and volcanic rocks based on thermodynamic and kinetic considerations," *Geochimica et Cosmochimica Acta*, vol. 48, no. 7, pp. 1523–1534, 1984.

[54] M. Sang *et al.*, "Structural styles and zircon ages of the South Tianshan accretionary complex, Atbashi Ridge, Kyrgyzstan: Insights for the anatomy of ocean plate stratigraphy and accretionary processes," *Journal of Asian Earth Sciences*, vol. 153, pp. 9–41, 2018.

[55] E. Garzanti and A. Resentini, "Provenance control on chemical indices of weathering (Taiwan river sands)," *Sedimentary Geology*, vol. 336, pp. 81–95, 2016.

[56] L. Harnois, "The CIW index: a new chemical index of weathering," *Sedimentary Geology*, vol. 55, no. 3, pp. 319–322, 1988.

[57] C. M. Fedo, H. Wayne Nesbitt, and G. M. Young, "Unraveling the effects of potassium metasomatism in sedimentary rocks and paleosols, with implications for paleoweathering conditions and provenance," *Geology*, vol. 23, no. 10, pp. 921–924, 1995.

[58] R. A. Obasi and H. Y. Madukwe, "Use of geochemistry to study the provenance, tectonic setting, source-area weathering and maturity of Igarra Marble, Southwest, Nigeria," *American Journal of Engineering Research, 5 (6), 90*, vol. 99, 2016.

[59] N. A. Etemad-Saeed, M. A. Hosseini-Barzi, and J. S. Armstrong-Altrin, "Petrography and geochemistry of clastic sedimentary rocks as evidence for provenance of the Lower Cambrian Lalun Formation, Posht-e-badam block, Central Iran," *Journal of African Earth Sciences*, vol. 61, no. 2, pp. 142–159, 2011.

[60] A. S. M. Sayem *et al.*, “Sedimentary and geochemical evidence of Eocene climate change in the Xining Basin, northeastern Tibetan Plateau,” *Science China Earth Sciences*, vol. 61, no. 9, pp. 1292–1305, 2018.

[61] L. J. Suttner and P. K. Dutta, “Alluvial sandstone composition and paleoclimate; I, Framework mineralogy,” *Journal of sedimentary Research*, vol. 56, no. 3, pp. 329–345, 1986, doi: 10.1306/212f8909-2b24-11d7-8648000102c1865d.

[62] R. Cox, D. R. Lowe, and R. L. Cullers, “The influence of sediment recycling and basement composition on evolution of mudrock chemistry in the southwestern United States,” *Geochimica et Cosmochimica Acta*, vol. 59, no. 14, pp. 2914–2940, 1995.

[63] F. J. Pettijohn, P. E. Potter, and R. Siever, “Introduction and source materials,” in *Sand and sandstone*, Springer, 1987, pp. 1–21.